University of North Carolina at Asheville
Journal of Undergraduate Research
Asheville, North Carolina
December 2013

QTAIM Studies of the C-Si Bonding in Geometrically Non-Classical Chlorofluorosilenes

Christian Williams
Chemistry
The University of North Carolina at Asheville
One University Heights
Asheville, North Carolina 28804 USA

Faculty Advisors: Dr. George Heard and Dr. Bert Holmes

Abstract

A likely pathway of decomposition of halosilanes in the upper atmosphere is 1,2-HX elimination, leading to a species following the form SiX_2CY_2(X and/or Y=F and/or Cl). While some of these molecules are predicted to be planar using ab initio and DFT methods, geometry optimizations of several of these species leads to a non-classical trans-bent structure confirmed by using multiple levels of theory. In order to probe the nature of bonding in these trans-bent geometries, Quantum Theory of Atoms in Molecules (QTAIM) was employed using electron densities generated at the same level of theory as optimization. The Laplacian of the electron density shows critical points indicative of regions of high electron localization-bonding electron domains and non-bonding electron domains. The presence of two unusual critical points above and below the near plane of the molecule, along with the longer than expected C-Si bond strongly suggest a single bond with singlet-biradical character of the two electrons not used in bonding. Compounds with a planar geometry lack these two unusual critical points and have a shorter C-Si bond length. This proposed singlet-biradical species is a new theory to explain trans-bending within molecules.

1. Introduction

1.1 Halogenated Silanes And Their Relation to Chlorofluorocarbons(CFCs) and Hydrochlorofluorocarbons(HCFCs)

It has long been established that chlorofluorocarbons(CFCs) and their close derivatives hydrochlorofluorocarbons(HCFCs) play a major role in the depletion of ozone in the atmosphere and contribute to global warming. Halogenated silanes, compounds containing both silicon and halogen atoms, potentially pose a similar threat but have been studied little for their global warming and ozone depletion potential when compared to CFC and HCFCs. The importance of understanding the fundamental reactions that happen to these molecules in the atmosphere cannot be understated. With the assemblage of data in regards to halogenated silanes having potential environmental risks or potential environmental benefits, conclusions may be made that effect either the future utilization or legislative banning of these compounds. Considering CFCs and HCFCs can bear close resemblance to halogenated silanes, our previous studies of CFCs and HCFCs can be used as a starting point for the extensive and rigorous study of these potential environmental degraders.

1.2 The Propagation of Halogenated Silanes into the Atmosphere

Understanding how silanes enter the atmosphere can be one potential way to reduce silane's effects on the environment. Silanes are used heavily in industrial processes that synthesize crystalline silicon which is then utilized

for different applications such as the manufacturing of semiconductors and solar cells. These industries use the process known as chemical vapor deposition (CVD) to form thin layers of silicon film in order to make their silicon semiconductors, circuits, and solar cells. To show an example of how much silane is used in the production of photovoltaic cells, about 2 kg of polysilicon is required to make a solar cell module of 6 × 12 cells with each cell being 125mm × 125mm. The amount of trichlorosilane ($HSiCl_3$) to make 1 kg of polysilicon, where the polysilicon would be used for the solar cell module stated above, is on the order of 11.3 kg.[1]

In the process of CVD, a film chamber is sealed and allowed to fill with the gas of choice in order to make the film or wafer. Once the gas is introduced into the chamber, which also contains a substrate for the silicon film to grow on, the temperature is increased to initiate the deposition reaction. It has been shown that most industries that need to produce some form of crystalline silicon use silane (SiH_4), dichlorosilane (H_2SiCl_2), and trichlorosilane ($HSiCl_3$).This is where the concern for analogous properties to known CFC and HCFCs comes into play. When the film deposition process is complete, silanes are purged from the chamber in order to retrieve the film. The purging is necessary because the deposition process does not possess complete reaction efficiency and thus has unreacted silane still present. Silanes from the CVD process that escape into the atmosphere pose a possible threat to the environment and should thus be studied in greater detail for any potential environmental risks.

1.3 Previous Experimental and Computational Research on Silanes and Halosilanes

Computationally, silanes have been investigated in many studies[2, 3] that research the bond angles and lengths of the molecules as well as bond energies, molecular energies, and transitions states of various intermediate structures. Ottosson and Eklöf reported data gathered by Bailleux et al. on the planar parent silene $H_2Si{=}CH_2$, and found that the Si=C bond length was 1.7039(18) Å.[4]This data is useful for comparing the molecules being researched here. However, studies such as the DFT experiments by Wang et al. have been done on halogenated silanes, cations, and radicals that have been identified in the CVD process that could be potentially useful information to change the parameters of the CVD of halogenated silanes[5] in order to streamline the process and increase the efficiency and thus lower environmental impacts. Levels of theory such as DFT were used in the present study among many others in order to ensure the presented optimized geometries were not specifically bound to DFT alone. Throughout the literature on the computational methods used in previous silane research, it has been found that various levels of theory have been used with basis sets yet to be tried in our research; therefore, many possible avenues of computational research may be yet followed.

Through reviewing the experimental literature, work done by Shuman et al.[6] involves some useful experimental thermochemical data on the heats of formation and bond dissociation energies of substituted chlorosilanes. Also, the work that was done by Shuman et al. gives experimental thermochemistry values that the authors compare with theoretical calculations done on similar halogenated silane molecules. This link between experimental and computational values has great promise in contributing to the expansion of the research of halogenated silanes. However, there is a limited quantity of experimental thermodynamic data available for the halosilanes, methylhalosilanes, and halomethylsilanes in terms of their heats of formation and bond dissociation energies (BDEs),[7]with the Shuman article being one of few, which could also be of use in supplying useful existing research information on the bonds breaking and forming.

1.4 The Trans-Bent Geometry

The original aim of this work was to investigate 1,2-HX elimination reactions of the halosilane trichloro(difluoromethyl)silane (CF_2HSiCl_3). The initial geometry of $CF_2HSiCl_3$was optimized as a ground state molecule whereby the H-Cl elimination transition state of CF_2HSiCl_3 could be compared. Surprisingly, the H-Cl elimination transition state from CF_2HSiCl_3 led to a CF_2SiCl_2 product which displayed non-classical trans-bent behavior. An IRC calculation was run on this transition state and was indeed verified as the true HCl elimination transition state. This initial indication of trans-bending behavior in halogenated silenes lead to the present study.

1.5 The Quantum Theory of Atoms in Molecules (QTAIM)

The fundamental property that Quantum Theory of Atoms in Molecules (QTAIM) is based upon is the electron density (ρ) of molecules. Electron density analysis of molecules results in the ability to visualize the contribution of electron density from every atom within the molecule. An atom within a molecule is partitioned from the rest of the

system (and thus its electron density contribution) via bond critical points and inter-atomic surfaces. Bond critical points within a molecule represent the point along the electron density interaction path (a gradient vector) in which the electron density is at a local minimum between two atoms. Moving along either side of the bond critical point corresponds to increasing electron density towards either atom characterized by that electron density path interaction. The research presented here is in a specific property built off of the electron density within tetra-halogenated Si-C systems. The laplacian ($\nabla^2\rho$) of electron density is capable of representing electronic charge concentration and depletion beyond the core of atoms. This QTAIM function allows the capability of visualizing points in the overall valence region (known in QTAIM vocabulary as the Valence Shell Charge Concentration or VSCC) within a molecule that represent maxima or minima in electronic charge concentration or electronic charge depletion. The laplacian of electron density within these molecules allow for a more thorough analysis of the structure and location of electron density.

1.6 Objectives of Research

In this research, the QTAIM analysis of tetrahalosilene molecules was executed in order to clearly understand the electron density present within these molecules and how the laplacian of the electron density ($\nabla^2\rho$) within these molecules can explain their geometric distortions. Once there is a clear understanding of the electronic environment of these molecules, research will continue on this family of molecules in order to make comparisons with molecules exhibiting similar geometric properties. This data will be used to try and make connections with how the electronic environment of these molecules can impact potential decomposition reactions that can in turn be compared with data on CFC's and HCFC's.

2. Computational Methods

Every combination of the SiX_2CY_2 (X and/or Y=F and/or Cl) system was optimized in Gaussian 09 under the following levels of theory: B3PW91[8], MP2[9], MP4(SDQ)[10], CCSD[11], and QCISD[12]. The basis set 6-311+G(2d) 6d 10f was used for each level of theory during the optimizations for each of the molecules presented here. Optimizations were carried out for both singlet and triplet geometries. When a molecule was optimized, the vibrational frequencies were analyzed to determine if the optimized geometry represented either a ground state or transition state geometry. If the geometry optimized exhibited one imaginary frequency, this would mean the molecule's optimized geometry was a transition state.

From each optimized geometry under each level of theory, wavefunction files were made with the same levels of theory and basis sets. These wavefunction files are the files that directly link the calculations done through Gaussian and the electron density calculations done through AIMAll[13].AIMStudio was used as a visualization tool to help in identifying the laplacian of the electron density. With the laplacian of electron density, electron localization (corresponding to (3,+3) critical points in the valence shell charge concentration (VSCC) of the atoms within the molecule) can be identified. Using the various programs within AIMAll, electron density (ρ) graphs were analyzed from each optimized molecule in conjunction with laplacian of the electron density ($\nabla^2\rho$) analysis. From the $\nabla^2\rho$ analysis, various critical points signifying local maxima in electron localization are able to be viewed. Isosurface graphs for each molecule were made in order to visualize the$\nabla^2\rho$ analysis of each molecule.

3. Results

3.1 Gaussian Analysis and Molecular Geometries

There are ten molecules that have been researched and all have combinations of chlorine and fluorine atoms attached to a silicon-carbon backbone. The specific formulas for these molecules are as follows: CF_2SiCl_2, CCl_2SiF_2, (E)-CClFSiClF, (Z)-CClFSiClF, $CClFSiCl_2$, $CFClSiF_2$, CCl_2SiClF, CF_2SiFCl, CCl_2SiCl_2, and CF_2SiF_2. The optimized CF_2SiCl_2 molecule had zero imaginary frequencies and thus was determined not to be a transition state geometry. The optimized output molecule can be seen in Figure1.

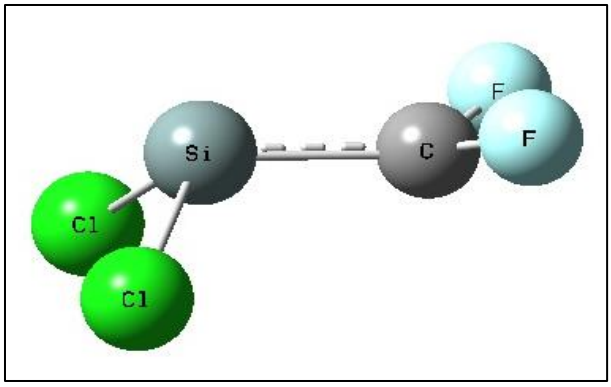

Figure 1. Product (excluding the HCl) from the elimination of HCl from CF_2HSiCl_3

Figure 1 As an elimination product, it is expected the geometry of CF_2SiCl_2 be planar. However the non-classical trans-bent nature of the optimized CF_2SiCl_2 initiated research into the tetrahalosilenes presented here

One can notice from Figure 1 that even with four substituents on the silicon carbon backbone, the expected planar geometry of the molecule is not observed. Instead, a distinct non-planar geometry exhibiting trans-bent behavior was found about the Si-C bond. When each of these molecules were optimized using a multiplicity of 3, that is, the molecule in the input file was assigned to have two unpaired electrons, the bent geometry was retained, but the molecules adopted a staggered arrangement about the central silicon-carbon axis.

Forced planar geometries of these molecules were also optimized in Gaussian for confirmation that the trans-bent molecules being presented were indeed the lowest energy geometrical atomic configuration. The majority of the set of molecules listed above were shown to exhibit one imaginary frequency if optimized to a forced planar geometry while zero imaginary frequencies were found for the trans-bent structures. A complete table of the preferred optimized geometry identities of the silene molecules can be seen in Table 1 along with the values of the Si-C bond lengths. It should be noted that these are the geometries that showed no imaginary frequencies and thus represent ground state geometries.

Table 1. Carbon-Silicon bond lengths for the ten molecules studied at each level of theory. All values given optimized using 6-311+G(2d) 6d 10f basis set

Levels of Theory	**CF_2SiF_2 C-Si bond length (Å)**	**CF_2SiFCl C-Si bond length (Å)**	**CF_2SiCl_2 C-Si bond length (Å)**	**$CFClSiF_2$ C-Si bond length (Å)**	**CCl_2SiCl_2 C-Si bond length (Å)**
B3PW91	1.87198	1.84074	1.81786	1.79672	1.70803
MP2	1.82401	1.80502	1.79223	1.76995	1.71051
MP4(SDQ)	1.84611	1.82137	1.80196	1.79395	1.70481
CCSD	1.84806	1.82205	1.80172	1.78473	1.70343
QCISD	1.86128	1.83263	1.80944	1.79150	1.70436
Preferred Geometry	Trans-bent	Trans-bent	Trans-bent	Trans-bent	Planar
Levels of Theory	**CCl_2SiClF C-Si bond length (Å)**	**CCl_2SiF_2 C-Si bond length (Å)**	**$CClFSiCl_2$ C-Si bond length (Å)**	**E-CClFSiClF C-Si bond length (Å)**	**Z-CClFSiClF C-Si bond length (Å)**
B3PW91	1.69976	1.70082	1.75956	1.77498	1.77511
MP2	1.70240	1.69544	1.75996	1.76259	1.76353
MP4(SDQ)	1.69785	1.69102	1.75978	1.77492	1.77542
CCSD	1.69660	1.69085	1.74849	1.76473	1.76516
QCISD	1.69747	1.69122	1.75032	1.76848	1.76889
Preferred Geometry	Planar	Planar	Trans-bent	Trans-bent	Trans-bent

As shown from Table 1, a peculiar trend can be seen with the increasing number of chlorine atoms present in the molecule, specifically on the carbon atom, bond lengths are shorter compared to the molecules with carbons having at least one fluorine atom. The bond lengths associated with these planar optimized geometries also exhibit the bond length closest to that of the parent silene.

A measure of the degree of trans-bending is the dihedral or torsional angle- the bond angle between the Si-X and C-X bonds. In a planar geometry, this angle is 0˚, and in a tetrahedral (sp^3) geometry, this angle would be 60˚. A further trend may be noticed in Tables 2-9 where dihedral bond angles are given for all molecules under each level of theory.

Table 2.**Left**: Dihedral angles of CF_2SiF_2, **Right**: Dihedral angles of CF_2SiCl_2

	CF_2SiF_2	F-C-Si-F Dihedral Angles (˚)		**CF_2SiCl_2**	F-C-Si-Cl Dihedral Angles(˚)
Levels of Theory	B3PW91	53.21303		B3PW91	45.05442
	MP2	48.95839		MP2	41.51582
	MP4(SDQ)	51.32479		MP4(SDQ)	43.27464
	CCSD	51.46311		CCSD	43.21147
	QCISD	52.38644		QCISD	44.17924

Table 3. Dihedral angles of CF_2SiFCl

	CF_2SiFCl	F-C-Si-F Dihedral Angles (˚)	F-C-Si-Cl Dihedral Angles (˚)
Levels of Theory	B3PW91	45.59728	52.88028
	MP2	42.23294	48.20021
	MP4(SDQ)	44.30617	50.70558
	CCSD	44.49759	50.60498
	QCISD	45.36903	51.73709

Table 4. Dihedral angles of CFCl SiF_2

	$CFClSiF_2$	F-C-Si-F Dihedral Angles(˚)	Cl-C-Si-F Dihedral Angles(˚)
Levels of Theory	B3PW91	44.43287	45.09732
	MP2	38.7861	39.8504
	MP4(SDQ)	43.32151	44.51629
	CCSD	42.20661	43.12947
	QCISD	43.18325	44.17096

Table 5.**Left:** Dihedral angles of CCl_2SiCl_2, **Right:** Dihedral angles of CCl_2SiF_2. Note for CCl_2SiF_2 at B3PW91, the large deviation from 0 indicates that, to a very small degree, the optimized geometry of CCl_2SiF_2 is trans-bent

	CCl_2SiCl_2	Cl-C-Si-Cl Dihedral Angles(˚)		**CCl_2SiF_2**	Cl-C-Si-F Dihedral Angles(˚)
Levels of Theory	B3PW91	0.05219		B3PW91	14.90554*
	MP2	0.07279		MP2	0.24521
	MP4(SDQ)	0.01212		MP4(SDQ)	0.05333
	CCSD	0.00066		CCSD	0.01906
	QCISD	0.00346		QCISD	0.0101

Table 6. Dihedral angles of $CClFSiCl_2$

	$CClFSiCl_2$	Cl-C-Si-Cl Dihedral Angles (˚)	F-C-Si-Cl Dihedral Angles(˚)
Levels of Theory	B3PW91	34.50378	33.02747
	MP2	33.85584	31.91487
	MP4(SDQ)	34.75464	32.62096
	CCSD	31.78124	29.86834
	QCISD	32.34241	30.32666

Table 7. Dihedral angles of CCl_2SiClF

	CCl_2SiClF	Cl-C-Si-F Dihedral Angles(˚)	Cl-C-Si-Cl Dihedral Angles(˚)
Levels of Theory	B3PW91	0.15989	0.04461
	MP2	0.12354	0.12807
	MP4(SDQ)	0.06344	0.04088
	CCSD	0.07789	0.06401
	QCISD	0.06735	0.05029

Table 8. Dihedral angles of E-CClFSiClF

	E-CClFSiClF	Cl-C-Si-F Dihedral Angles(˚)	F-C-Si-Cl Dihedral Angles(˚)
Levels of Theory	B3PW91	37.08164	42.21895
	MP2	34.1628	37.72858
	MP4(SDQ)	37.21819	41.35229
	CCSD	35.48237	39.31831
	QCISD	36.20708	40.11969

Table 9. Dihedral angles of Z-CClFSiClF

	Z-CClFSiClF	Cl-C-Si-Cl Dihedral Angles(˚)	F-C-Si-F Dihedral Angles(˚)
Levels of Theory	B3PW91	43.26357	35.74115
	MP2	39.21105	32.77457
	MP4(SDQ)	43.03065	35.5001
	CCSD	40.69035	33.98829
	QCISD	41.55388	34.63849

Tables 2-9. Dihedral angles for the trans-bent molecules are larger than those for the planar molecules. The correlation between dihedral angles and the degree of "trans-bentness" is as follows: the larger the dihedral angles, the greater the degree of trans-bending.

From tables 2-9, the main aspect that can be taken away is that for the molecules that have higher dihedral angles, this correlates to the same molecules having a greater degree of trans-bending. Across all levels of theory, the molecules containing trans-bent behavior all have dihedral angles around the same range. The consistency of the dihedral angles to a similar range across levels of theory means that the trans-bending behavior is well established and that the behavior is not an artifact of a single level of theory within computational chemistry. The geometric peculiarities given by the Gaussian analysis of the tetrahalosilene molecules studied necessitated the AIMAll analysis of the same molecules including the laplacian of the electron density ($\nabla^2\rho$) and isosurface graphs.

3.2 Laplacian of Electron Density ($\nabla^2\rho$) and Isosurface Graphs

The AIMAll analysis of the tetrahalosilenes discussed are presented in Figures 2-11. As can be seen from these figures, a wide range of laplacian (3,+3) critical points can be seen in the pictures on the left. Critical points represent regions of localization and correspond to bonding electrons and lone pairs. This discussion will focus on critical points in the region between the Si and C atoms. Two isolated critical points, above and below the carbon-silicon plane, represent areas of electron localization. In the planar molecules, given in Table 1, no such spatial

orientation of electron localization maxima is present above and below the C-Si bond plane. Instead, a maxima in electron localization is directly in the bond of silicon to carbon which is consistent with a bonding electron pair. To visualize the electron density localization with more detail, isosurface graphs for some of the molecules presented here can be seen in Figures 2-11. From the isosurface plots of the trans-bent molecules, there is a clear 'cap-shaped' region of electron localization on the silicon atom below the plane of the molecule. These caps coincide with the (3,+3) laplacian critical point on the silicon atom of the same molecule in Figures 2-11. The cap on the carbon atom is actually combined with the electron density between the carbon and silicon atoms and can be seen in the isosurface graphs of Figure 6 as a bulge in the area above the carbon atom. The isosurface graph for the planar molecules can be seen in Figures 7,8, and 9. The isosurface graphs corroborate their corresponding laplacian (3,+3) critical points in that there are no stray "caps" present within the molecules.

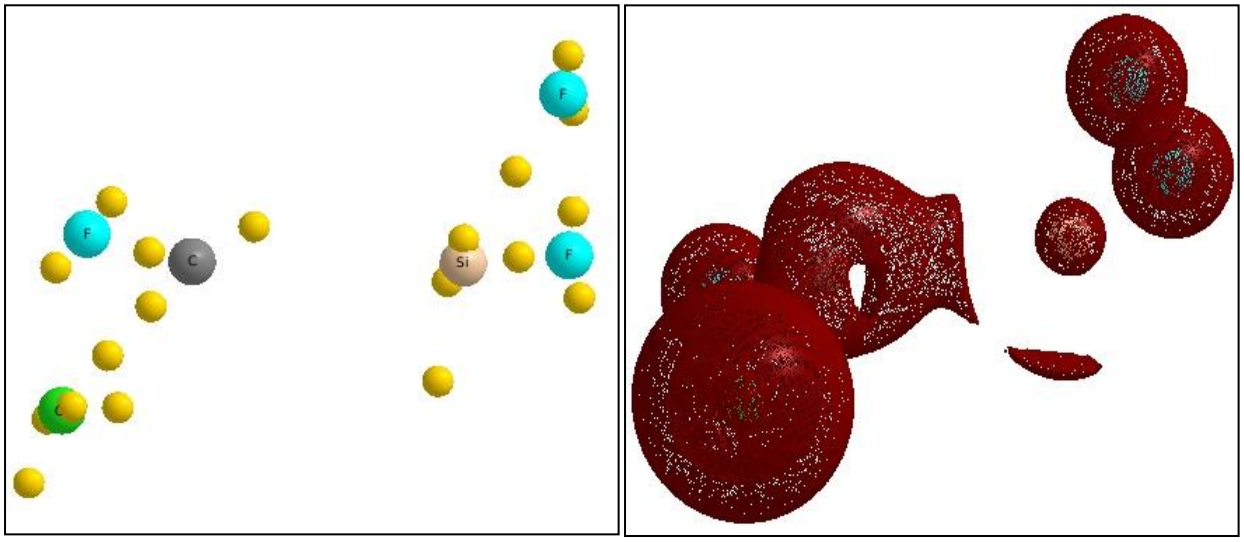

Figure 2.**Left:** Laplacian (3,+3) critical points of trans-bent $CFClSiF_2$
Right: Isosurface graph of trans-bent $CFClSiF_2$ ($\nabla^2\rho$=-0.09)

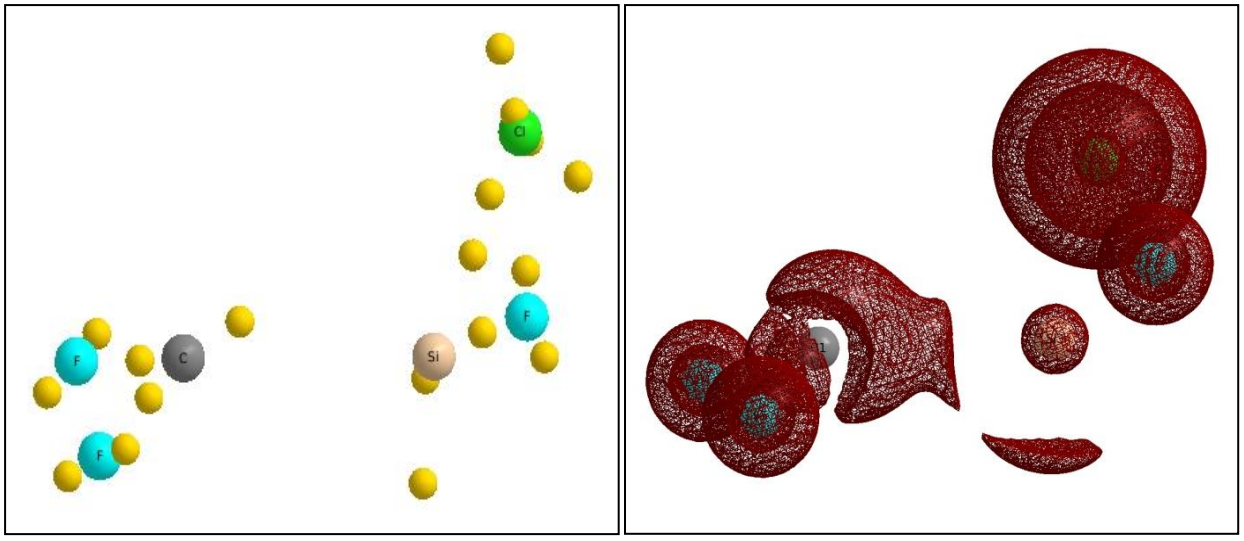

Figure 3.**Left:** Laplacian (3,+3) critical points of trans-bent CF_2SiFCl
Right: Isosurface graph of trans-bent CF_2SiFCl ($\nabla^2\rho$=-0.08)

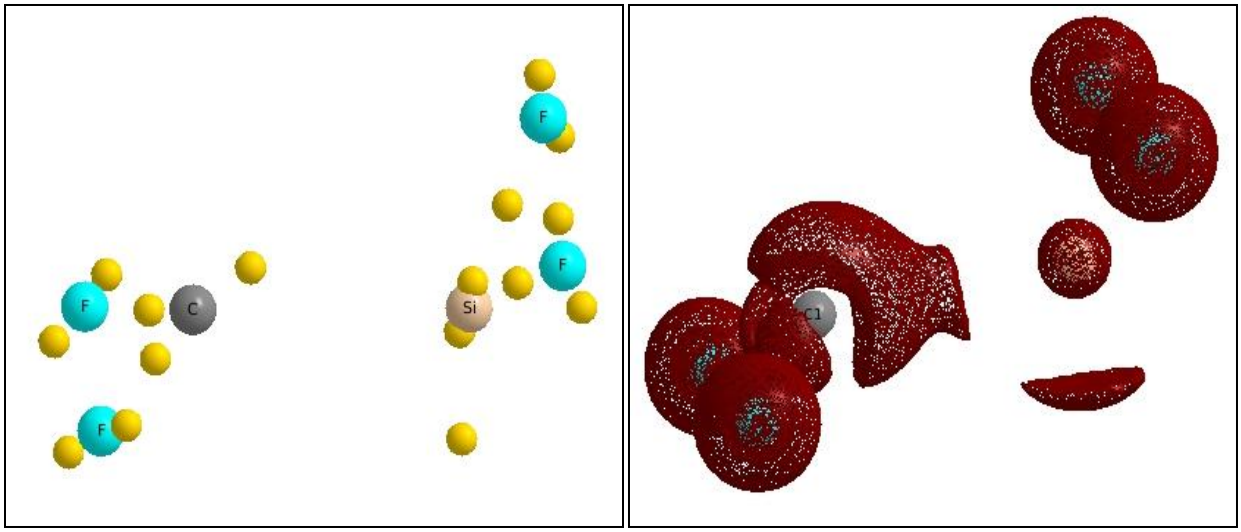

Figure 4.**Left:** Laplacian (3,+3) critical points of trans-bent CF_2SiF_2
Right: Isosurface graph of trans-bent $CFClSiF_2(\nabla^2\rho=-0.09)$

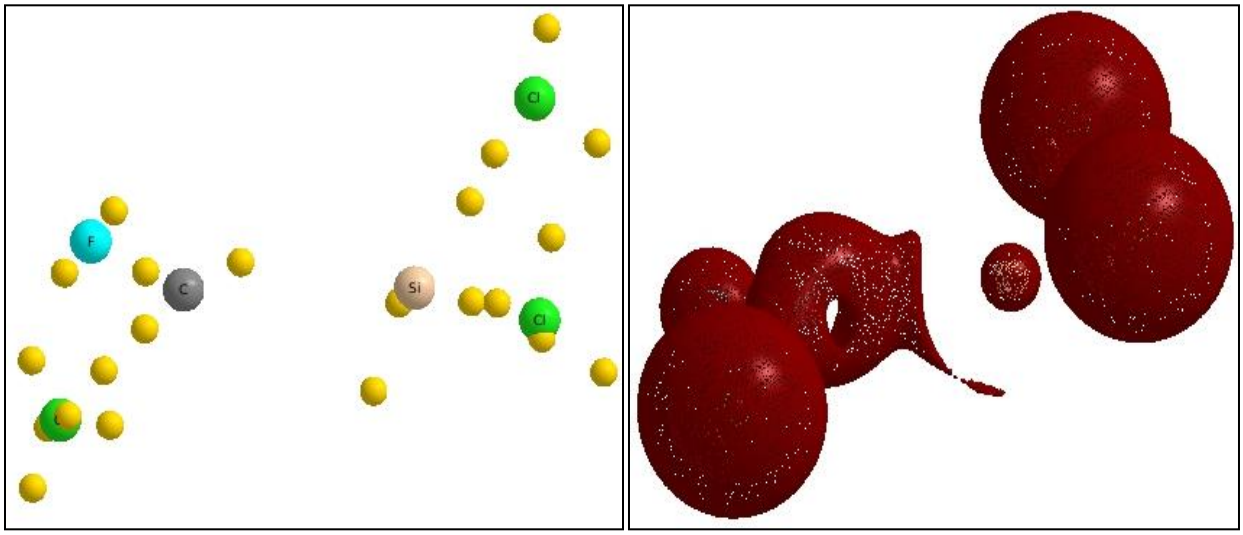

Figure 5.**Left:** Laplacian (3,+3) critical points of trans-bent $CFClSiCl_2$
Right: Isosurface graph of trans-bent $CFClSiCl_2(\nabla^2\rho=-0.08)$

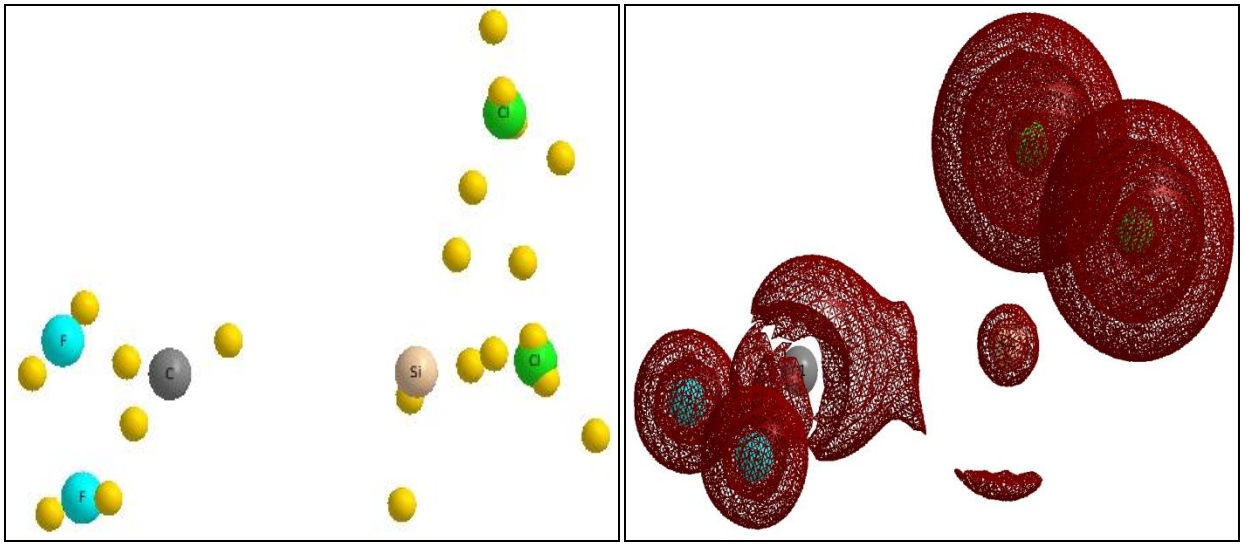

Figure 6. **Left:** Laplacian (3,+3) critical points of trans-bent CF_2SiCl_2
Right: Isosurface graph of trans-bent CF_2SiCl_2 ($\nabla^2\rho$=-0.08)

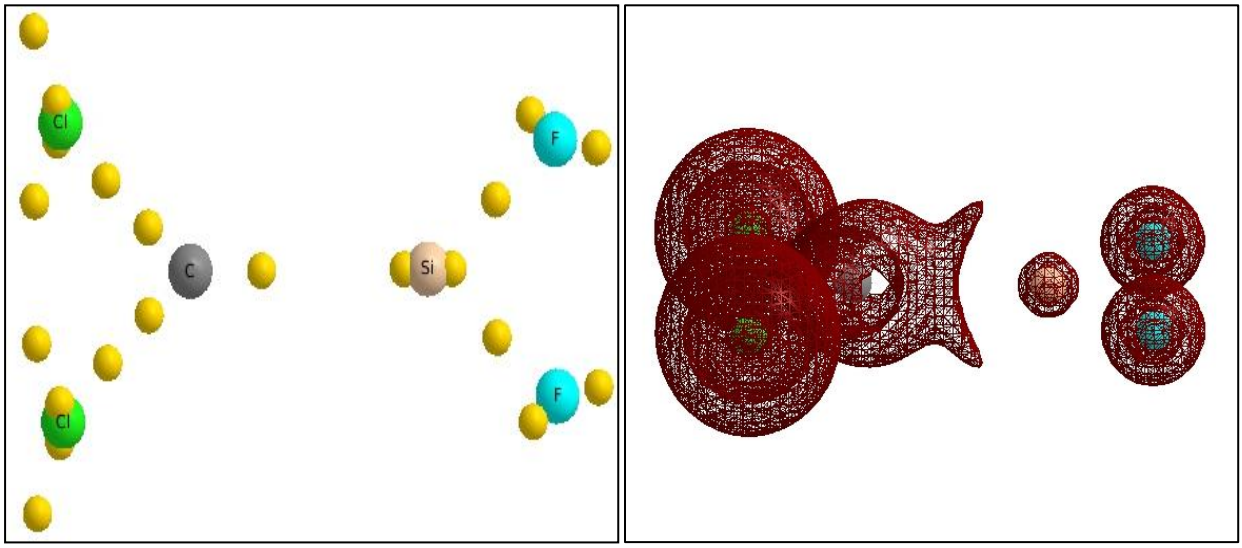

Figure 7.**Left:** Laplacian (3,+3) critical points of planar CCl_2SiF_2
Right: Isosurface graph of planar CCl_2SiF_2 ($\nabla^2\rho$=-0.08)

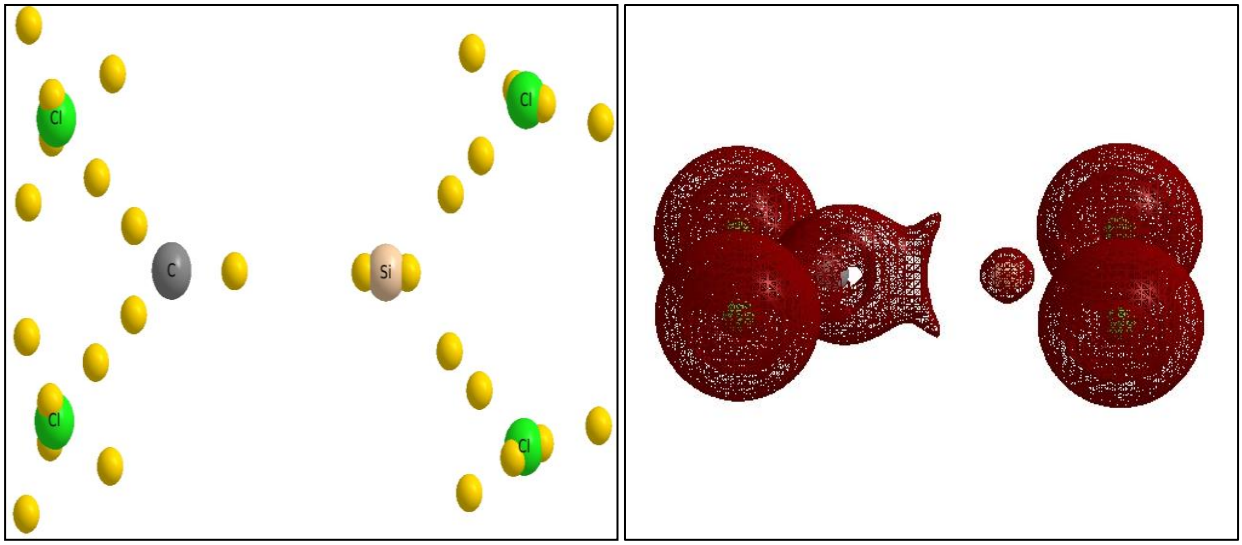

Figure 8. **Left:** Laplacian (3,+3) critical points of planar CCl_2SiCl_2
Right: Isosurface graph of planar CCl_2SiCl_2 ($\nabla^2\rho$=-0.08)

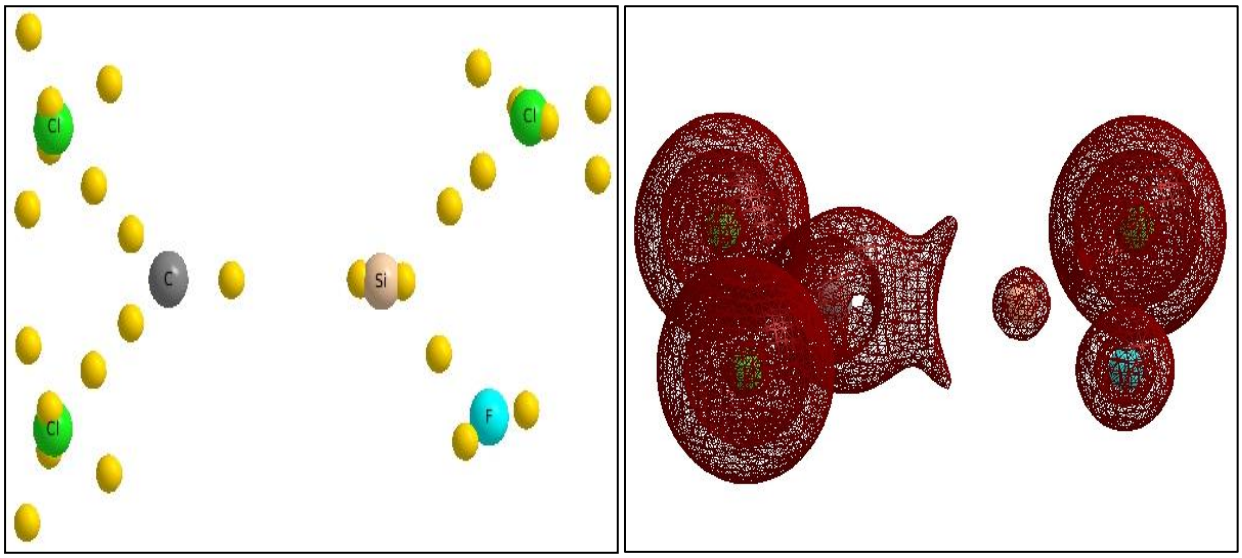

Figure 9.**Left:** Laplacian (3,+3) critical points of planar CCl_2SiClF
Right: Isosurface graph of planar CCl_2SiClF ($\nabla^2\rho$=-0.08)

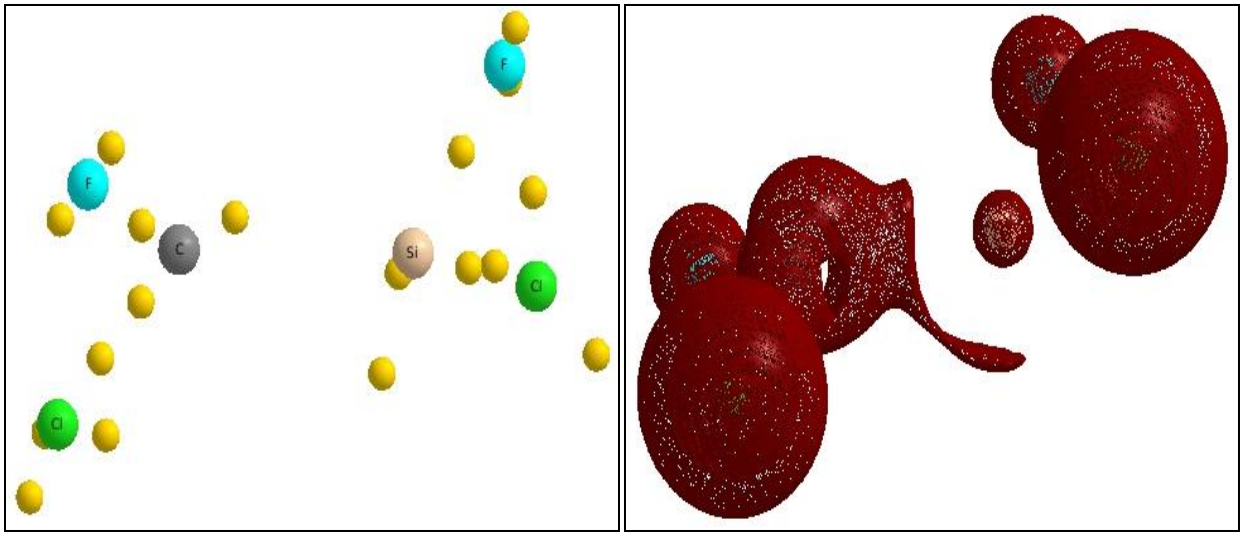

Figure 10.**Left:** Laplacian (3,+3) critical points of trans-bent Z-CClFSiClF
Right: Isosurface graph of trans-bent Z-CClFSiClF ($\nabla^2\rho$=-0.08)

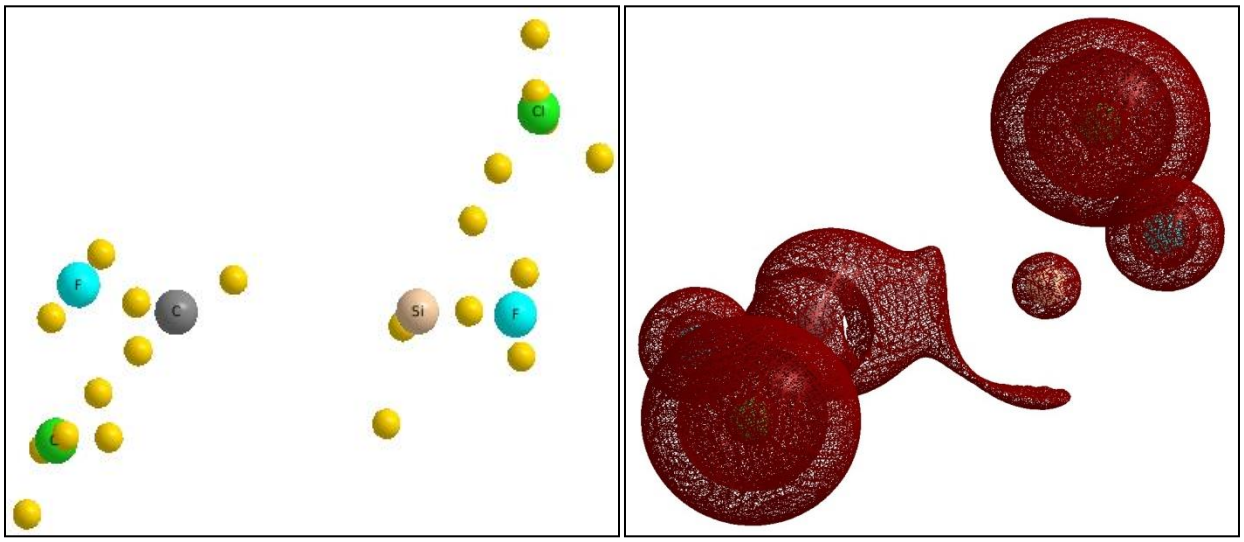

Figure 11.**Left:** Laplacian (3,+3) critical points of trans-bent E-CClFSiClF
Right: Isosurface graph of trans-bent E-CClFSiClF ($\nabla^2\rho$=-0.08)

Figures 2-11 The laplacian (3,+3) critical points on the left sides of each figure represents a local maxima in electron localization. The interesting critical points are those out of the C-Si bond plane, namely, the critical point to the upper-right of the carbon atom and the critical point to the lower left of the silicon atom. The planar-preferred molecules do not have these isolated (3,+3) critical points. Right side pictures are isosurface graphs representing more three-dimensionally the localization of electron density by having "caps" corresponding to the two interesting critical points described above.

Notice in the figures with the trans-bent molecules that a critical point is present above and slightly to the right of the carbon atom and a critical point is also present below and to the left of silicon. Here again it is found that when comparing these unique out of plane critical points between trans-bent molecules, they are similar in both location and size. In the planar molecules, given from Table 1, no such spatial orientation of charge maxima is present in their laplacian critical point pictures on the left. Instead, a critical point in electron localization is directly in the bond of silicon to carbon.

From the isosurface plots of the trans-bent molecules of Figures 2-11, there is a clear cap on the silicon atom placed below the molecule. This cap coincides with their corresponding (3,+3) laplacian critical point on the silicon atom. The cap on the carbon atom is actually combined with the electron density between the carbon and silicon atoms and can be seen in the isosurface graphs of the trans-bent molecules in Figures 2-11 as a bulge in the area above the carbon atom. In the planar molecules, these caps are not found and can be said that this is due to the absence of their trans-bending behavior.

4. Discussion

It is clear from these results that there is electron localization above and below the carbon-silicon bond plane. Such localization cannot be accounted for using traditional bonding ideas. Through QTAIM precedents, these areas of electron localization are in the valence shell of the carbon and silicon atoms. Common bonding descriptions are based on orbital concepts such as hybridization. Hybridization, however, would lead to a different picture of localization in these molecules. Considering this, the theory to describe the bonding found in these molecules should move away from orbital-based models. The results of this work point strongly to a single bond through the bond path between carbon and silicon, the bond distances, and a singlet-biradical interaction of the other two electrons as represented by two isolated $\nabla^2\rho$ maxima as shown in Figure 12.

As an important aspect to the QTAIM, Bader et al. had discovered that the Laplacian of the electron density provided a remarkable mapping of the number and properties of the localized electron pairs assumed in the VSEPR model of molecular geometry on to the number and properties of the local maxima found in the VSCC of an atom.[14]The presentation of these molecules happens with the understanding of this analysis as being an orbital-free analysis, which inherently comes from the VSEPR aspect of the QTAIM. The existence of trans-bent structures has been previously found in chemistry. Lappert and co-workers discovered a trans bent structure of distannene $[Sn_2(CH(SiMe_3)_4]$ in the 1970's and proposed a double donor-acceptor bond[5] where one sp^2 tin atom would transfer an entire electron pair to the open p-orbital on the other tin atom and vice versa. Lappert suggested that this behavior would result in the trans-bent structure of distannene. However, this would leave no chance for any single bond to form due to the fact that no two electrons would be used to make a single bond between the tin atoms since whole electron pairs are being transferred. This theory does not fit with the fact that all of the molecules presented here had clear bonding paths between the central carbon and silicon atoms and this is supported by the bond lengths given in Table 1.

Another theory proposed for the trans-bent nature of molecules that are expected to be planar is the valence bond theory.[4] This theory asserts that between the two backbone atoms in the trans-bending molecules, a single electron pair is resonating. The valence bond theory also does not accurately fit the data presented for these tetrahalosilene molecules due to the existence of localized laplacian (3,+3) critical points placed on the carbon and silicon atoms. The isolated caps in the representative isosurface graphs in Figures 2-11 for the trans-bent molecules supports this incongruence with the valence bond theory. Further, under valence bond theory, the singlet and triplet optimized geometries would be similar whereas the results for these calculations showed drastic geometric differences when comparing the singlet and triplet geometry optimizations.

On a more thermodynamically based theory for the existence of trans-bent molecules is the Carter-Goddard-Malrieu-Trinquier (CGMT) theory. With CGMT theory, the onset of a trans-bent geometry within a molecule can be expressed by the inequality $\sum\Delta E_{ST} \geq \frac{1}{2}E_{\sigma+\pi}$ where $\sum\Delta E_{ST}$ is the sum of the energy differences between the singlet and triplet carbene or silylene fragments and $\frac{1}{2}E_{\sigma+\pi}$ is the total energy of the sigma and pi bonds between the two central atoms in the molecule which is then divided by two. According to CGMT theory, if this equality holds for molecules with the chance to either be planar or trans-bent, the trans-bent geometry would be favored over the planar geometry. When considering the data presented here, this thermodynamic inequality can also be considered outside of the true bonding nature of these particular halosilenes because of the large geometric changes that occurred between the multiplicity 1 and multiplicity 3 calculations within the same molecules.

Contributed here is a QTAIM method for analysis of trans-bent halogenated silenes. Electron localization can be used, through AIMAll analysis, to help visualize and provide data for a theory involving two critical points above and below the bond plane of the two central atoms in trans-bending molecules. The critical points would represent two isolated electrons, one associated with the carbon atom while the other is associated with the silicon atom, but both the carbon and silicon atom have a bonding interaction between them in conjunction with these isolated critical points in electron localization.

5. Conclusion

As the first conclusion that can be drawn from this data, a large number of halogenated formally silene species which were expected to display planar geometries actually exhibit trans-bent behavior across different levels of theory in computational chemistry. From the data provided here, another theory can be included to those in the discussion section. The trans-bent tetrahalosilene molecules presented can be described as representing singlet bi-radical species with a proposed structure of that in Figure 12.

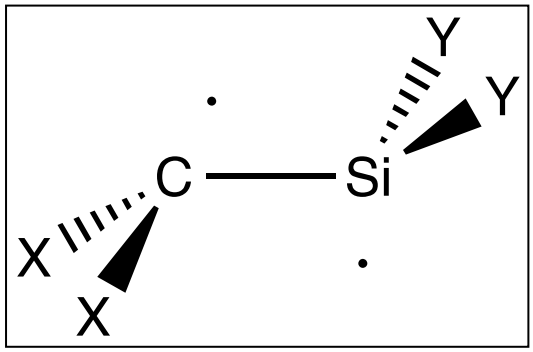

Figure 12. The proposed singlet bi-radical geometry of the trans-bent molecules presented

Figure 12 The localized electrons above and below the carbon-silicon bonding plane are said to be represented by the isolated laplacian (3,+3) critical points found in the trans-bent species in Figures 2-11. Here, X and Y could be fluorine and/or chlorine atoms but at least one X must be fluorine in order for trans-bent geometry to occur.

This singlet bi-radical theory is supported by the existence of bond interaction between the carbon and silicon atoms within these molecules and the clear localization of electron density uniquely spaced as represented in the trans-bent molecules found in Figures 2-11.

A further conclusion can be made about what molecules would be expected to exhibit this trans-bending behavior. It is indicated that molecules containing carbon atoms with at least one fluorine substituent will be trans-bending if the carbon is bonded to a silicon atom containing halogens. From the gathered data on trans-bent tetrahalosilenes, it is proposed that the onset of a trans-bent characteristic will occur in all tetrahalosilenes containing CF_2 or CFCl groups. This is supported by the data showing that all of the molecules having a CF_2or CFCl group were, to varying degrees, trans-bent.

5. Acknowledgments

The author would like to thank the National Science Foundation from which came the following research grants in order for this research to be accomplished: MRI CHE-1229406, RUI CHE-1111546. The author would also like to thank University of North Carolina at Asheville Undergraduate Research Program and the University of North Carolina at Asheville Chemistry Department

6. References

1. Fthenakis,V.M.; Kim, H.C. Photovoltaics: Life-cycle analyses, *Solar Energy.***2011**, *85*(8), 1609-1628.
2.Mains, G.J.; Trachtman, M.; Bock C.W.Transition States for Molecular Hydrogen Elimination from Substituted Silanes,*Journal of Molecular Structure (Theochem).***1991**, *231*, 125-136.
3. Islam, S.M.; Hollett, J.W.; Poirier, R.A.Computational Study of the Reactions of SiH3X (X = H, Cl, Br, I) with HCN, *J. Phys. Chem. A.* **2007**, *111*, 526-540.
4. Ottoson, H.; Eklöf, A.M. Silenes: Connectors between classicalalkenes and nonclassical heavy alkenes,*Coordination Chemistry Reviews.* **2008**, *252*,1287–1314.

5. Wang, L.; He, Y.L.Halogenated silanes, radicals, and cations: Theoretical predictions on ionization energies, structures and potential energy surfaces of cations, proton affinities, and enthalpies of formation,*International Journal of Mass Spectrometry*. **2008**,*276*(1),56-76.
6. Shuman, N.S.; Spencer, A.P.; Baer, T. Experimental Thermochemistry of $SiCl_3R$ (R= Cl, H, CH_3, C_2H_5, C_2H_3, CH_2Cl, $SiCl_3$), $SiCl_3^+$, and SiCl3•, *J. Phys. Chem. A.* **2009**, *113*, 9458–9466.
7. Grant, D.J.; Dixon, D.A. Heats of Formation and Bond Dissociation Energies of the Halosilanes, Methylhalosilanes, and Halomethylsilanes,*J. Phys. Chem. A.* **2009**, *113*, 3656–3661.
8. B3PW91
J. P. Perdew, in *Electronic Structure of Solids '91*, Ed. P. Ziesche and H. Eschrig (AkademieVerlag, Berlin, 1991) 11.
J. P. Perdew, J. A. Chevary, S. H. Vosko, K. A. Jackson, M. R. Pederson, D. J. Singh, and C. Fiolhais, "Atoms, molecules, solids, and surfaces: Applications of the generalized gradient approximation for exchange and correlation," *Phys. Rev. B*, **46** (1992) 6671-87.
J. P. Perdew, J. A. Chevary, S. H. Vosko, K. A. Jackson, M. R. Pederson, D. J. Singh, and C. Fiolhais, "Erratum: Atoms, molecules, solids, and surfaces - Applications of the generalized gradient approximation for exchange and correlation," *Phys. Rev. B*, **48** (1993) 4978.
J. P. Perdew, K. Burke, and Y. Wang, "Generalized gradient approximation for the exchange-correlation hole of a many-electron system," *Phys. Rev. B*, **54** (1996) 16533-39.
K. Burke, J. P. Perdew, and Y. Wang, in *Electronic Density Functional Theory: Recent Progress and New Directions*, Ed. J. F. Dobson, G. Vignale, and M. P. Das (Plenum, 1998).
9. MP2
M. Head-Gordon, J. A. Pople, and M. J. Frisch, "MP2 energy evaluation by direct methods," *Chem. Phys. Lett.*, **153** (1988) 503-06.
S. Saebø and J. Almlöf, "Avoiding the integral storage bottleneck in LCAO calculations of electron correlation," *Chem. Phys. Lett.*, **154** (1989) 83-89.
M. J. Frisch, M. Head-Gordon, and J. A. Pople, "Direct MP2 gradient method," *Chem. Phys. Lett.*, **166** (1990) 275-80.
M. J. Frisch, M. Head-Gordon, and J. A. Pople, "Semi-direct algorithms for the MP2 energy and gradient," *Chem. Phys. Lett.*, **166** (1990) 281-89.
M. Head-Gordon and T. Head-Gordon, "Analytic MP2 Frequencies Without Fifth Order Storage: Theory and Application to Bifurcated Hydrogen Bonds in the Water Hexamer," *Chem. Phys. Lett.*,**220** (1994) 122-28.
10. MP4(SDQ)
G. W. Trucks, J. D. Watts, E. A. Salter, and R. J. Bartlett, "Analytical MBPT(4) Gradients," *Chem. Phys. Lett.*, **153** (1988) 490-95.
G. W. Trucks, E. A. Salter, C. Sosa, and R. J. Bartlett, "Theory and Implementation of the MBPT Density Matrix: An Application to One-Electron Properties," *Chem. Phys. Lett.*, **147** (1988) 359-66.
11. CCSD
J. Cížek, in *Advances in Chemical Physics*, Ed. P. C. Hariharan, Vol. 14 (Wiley Interscience, New York, 1969) 35.
G. D. Purvis III and R. J. Bartlett, "A full coupled-cluster singles and doubles model - the inclusion of disconnected triples," *J. Chem. Phys.*, **76** (1982) 1910-18.
G. E. Scuseria, C. L. Janssen, and H. F. Schaefer III, "An efficient reformulation of the closed-shell coupled cluster single and double excitation (CCSD) equations," *J. Chem. Phys.*, **89** (1988) 7382-87.
G. E. Scuseria and H. F. Schaefer III, "Is coupled cluster singles and doubles (CCSD) more computationally intensive than quadratic configuration-interaction (QCISD)?," *J. Chem. Phys.*, **90** (1989) 3700-03.
12. QCISD
J. A. Pople, M. Head-Gordon, and K. Raghavachari, "Quadratic configuration interaction - a general technique for determining electron correlation energies," *J. Chem. Phys.*, **87** (1987) 5968-75.
13. AIMAll Version
AIMAll (Version 13.05.06), Todd A. Keith, TK Gristmill Software, Overland Park KS, USA, 2013 (aim.tkgristmill.com)
14. *Atoms in Molecules: A Quantum Theory*; Bader, Richard F. W., International Series of Monographs on Chemistry Series 22; Oxford University Press, New York, 1990, p. 275.